Jpn. J. Appl. Phys. Vol. 40 (2001) pp. 364–370
Part 1, No. 1, January 2001

Modal Analysis of Hollow Cylindrical Guided Waves and Applications

Hideo NISHINO, Sunao TAKASHINA, Fukutoshi UCHIDA, Mikio TAKEMOTO and Kanji ONO[1]
Faculty of Science and Engineering, Aoyama Gakuin University, Setagaya, Tokyo 157-8572, Japan
[1]*Department of Materials Science and Engineering, UCLA, Los Angeles, CA 90095-1595, USA*

(Received July 11, 2000; accepted for publication September 13, 2000)

Dispersion behavior of guided waves in hollow cylinders (cylindrical waves) was evaluated theoretically and experimentally. Observed dispersion behavior suggests an assignment, different from the traditional one, of longitudinal (L-), flexural (F-) and torsional (T-) modes which are consistent with Lamb waves and shear-horizontal (SH) mode waves. The L- and F-modes of the cylindrical waves have characteristics which are asymptotic to Lamb waves and to waves in a solid cylinder. Experimentally, wide-band cylindrical waves in aluminum pipes were generated using a laser-ultrasonic method. Wavelet transform of the cylindrical wave signals was utilized for time-frequency analysis in order to compare them with the theoretical dispersion curves. For the L(0, 1), F(1, 1), F(2, 1), L(0, 2), F(1, 2) and F(2, 2) modes of the cylindrical waves, which were efficiently excited, theoretical and experimental dispersion curves agree with each other.

KEYWORDS: ultrasonics, acoustic waves, hollow cylinder, guided waves, modal analysis, hollow cylindrical guided waves

1. Introduction

Hollow cylinders have many industrial uses, such as, hydraulic and pneumatic control lines, heat-exchanger and steam-generator tubes, chemical plant piping and oil and gas pipelines, etc. Various terms are used for these cylinders depending on their size and purpose, but we call all of them a pipe. To ensure pipe reliability, ultrasonic testing has been utilized effectively both before and during service and some test procedures with cylindrical waves have been developed.[1–10] Cylindrical waves, or guided waves in hollow cylinders, are anticipated to play more prominent roles for ultrasonic and acoustic emission (AE) inspection of pipes. However, their use is limited at present due to the complexity of multi-mode waves and the presence of circumferential modes. Quantitative analysis of these waves needs to be extended to the level of bulk waves and surface or plate waves.

Gazis[11] provided the theoretical basis of cylindrical waves and his characteristic frequency equation is useful for a computer-aided calculation of velocity dispersion. Many experimental studies followed. Fitch[12] generated several kinds of longitudinal (L-) and flexural (F-) mode cylindrical waves using a pair of narrow-band piezoelectric transducers and verified the experimental results in comparison with the theoretical dispersion of cylindrical waves. Silk and Bainton[1] showed that the generation efficiency of the L(0, 1) mode, an equivalent to the A_0 mode Lamb wave, was larger than that of the L(0, 2) mode, an equivalent to the S_0 mode Lamb wave. This feature is similar to the generation efficiency of Lamb waves. Alleyne and Cawley[2] showed that the relation between the flaw size in the circumferential direction and reflection coefficient of the L(0, 2) mode was essentially linear. They also devised[3] a transduction system for the generation of cylindrical waves utilizing 8 or 16 separate transducers around the circumference of a pipe, and succeeded in the selective generation of the F(8, 1) mode. Up to 100 m propagation of the L(0, 2) mode through butt welds and holding brackets was also confirmed[4] in an actual chemical plant piping (76 mm, schedule 40). This long distance propagation is due to a low energy leakage of the cylindrical waves. Lowe *et al*. showed[5] a mode conversion from the L(0, 2) mode to F(1, 3) mode[13] due to a slit-type flaw and determined the conversion ratio as a function of slit depth using both experimental and finite element methods. Greenspon theoretically treated[6,7] the cylindrical waves that leak their energy into an outside liquid. Similar theoretical computation was also reported by Rose *et al*.[8] It was shown experimentally that the attenuation of the L(0, 1) mode due to liquid loading[9] or a wet insulator[2] around the pipe was larger than that of the L(0, 2) mode. Nishino *et al*.[10] reported a new source location method of AE signals in a pipe, using a single transducer at the pipe end, which was based on the group velocity difference of L(0, 1) and F(1, 1) modes at a certain frequency.

In this paper, modal analyses of the cylindrical waves were considered based on the velocity dispersion. The velocity dispersion curves of the cylindrical waves and Lamb waves are compared for several modes. Wide band excitations of the cylindrical waves with a laser ultrasonic method and time-frequency analysis utilizing the wavelet transform were conducted for experimental verification.

2. Velocity Dispersion of Hollow Cylindrical Guided Waves

2.1 Modes and dispersion curves

Phase velocity of the cylindrical wave is deduced from the wave equation described in cylindrical coordinates with a stress-free boundary condition at the inner and outer surfaces of a pipe.[11] The cylindrical wave is divided into three modes due to the vibration phenomenon. These are L-, F- and torsional (T-) modes. The L-mode is an axially symmetric mode, which is often called as the breathing mode.[14] The F-mode has nonaxially symmetric vibration and the T-mode is the wave, which has a relatively large displacement in the circumferential direction. The three modes are described as L(0, m), F(n, m) and T(n, m), where n and m are the circumferential and radial (thickness) mode parameters, respectively. Schematic illustrations of circumferential modes are shown in Fig. 1. The number of nodes and loops in the circumference is represented by $2n$.

Meitzler[15] and Zemanek[16] classified all the high order modes in the circumference into the F-mode. In their classification, the T-mode has only the circumferential fundamental mode ($n = 0$) and the modes with nonzero n are considered as the F-modes. We propose here that the n-parameter of the T-mode is not limited to zero. By separating the higher order T-modes (with non-zero n-values) from the F-modes, we can consistently correlate the higher order T-modes as modes

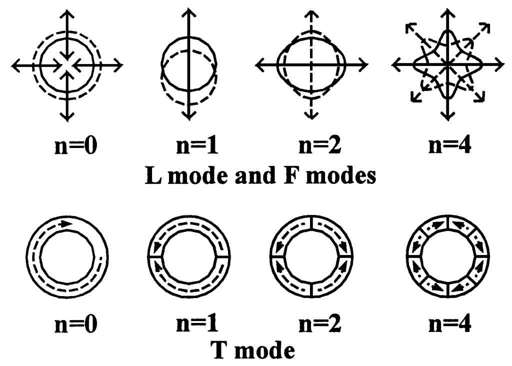

Fig. 1. Cross-sectional illustrations of circumferential vibration modes.

coupled only with shear horizontal mode (SH) waves at their cut-off frequencies (the so-called longitudinal shear waves in ref. 11). The cut-off frequencies of the modes are calculated from the following frequency equation.[11)]

$$J_n'(k_t a)Y_n'(k_t b) - J_n'(k_t b)Y_n'(k_t a) = 0, \qquad (1)$$

where J_n, Y_n, k_t, a and b are 1st and 2nd kind Bessel functions of n-th order, wave number of bulk shear wave, and outer and inner radii of the pipe, respectively. Table I shows the several lower order cut-off frequencies of the modes (using aluminum data for calculation). These values will be compared to the frequencies, at which the phase velocity of the T-mode takes an infinite value.

By adopting the presence of the higher order T-modes, the three modes (L-, F- and T-modes) can be interpreted due to the wave propagation phenomenon. The L- and F-modes have a very similar manner to the Lamb wave and the T-mode corresponds to the SH mode plate wave. That is to say, L- and F-mode are the guided waves mainly consisting of the bulk longitudinal and the bulk shear-vertical (SV) waves, and the T-mode mainly consists of the bulk SH wave.[14,17)] In the new classification, the two mode parameters, n and m, are simply related to vibration phenomena. When the m-parameter takes an odd or even number in the L- and F-modes, the vibration in the wall direction takes asymmetric or symmetric behavior, respectively. In addition, the modes labeled $m = 1$ and 2 (the L(0, 1), F(n, 1), L(0, 2) and F(n, 2) modes), which are equivalent to the A_0 and S_0 modes of the Lamb wave asymptotically approach the Rayleigh wave velocity (2840 m/s for aluminum) at a high frequency. This feature is based on the same reason why the A_0 and S_0 modes of the Lamb wave take the Rayleigh wave velocity at a high frequency.[17)] That is to say, the lowest two fundamental modes in the thickness direction in the Lamb and cylindrical waves take the Rayleigh wave velocity at a high frequency. This was not the case in the previous classification;[15,16)] the $F_p(n, 2)$ mode (subscript p denotes the previous classification) is asymptotic to the bulk shear wave velocity, while the $L_p(0, 1)$, $L_p(0, 2)$ and $F_p(n, 1)$ modes take the Rayleigh wave velocity at a high frequency. The $F_p(n, 2)$ and $F_p(n, 3)$ modes are classified into the T(n, 1) and F(n, 2) modes in our classification scheme, which provides consistency in the physical meaning. The particle displacement of the F(1, 2) mode (or $F_p(1, 3)$ mode in the previous assignment) was calculated and had symmetric distribution in the wall direction.[5)] This result also supports our classification scheme.

Figures 2(a) and 2(b) show phase and group velocity dispersions of the several lowest L- and F-modes of the cylindrical waves for an aluminum pipe of 5 mm diameter and 1 mm thickness ($c_l = 6400$ m/s, $c_t = 3040$ m/s). Thick dotted curves in Fig. 2 indicate the A_0, S_0 and A_1 Lamb wave dispersion curves for a 1-mm-thick aluminum plate, where plate thickness is equal to the wall thickness of the pipe considered. When the thickness/diameter (t/d) ratio of a pipe is the same, the shape of the dispersion curve is identical regardless of the changes in t or d. However, the horizontal frequency

Table I. Cut-off frequencies of fundamental and high order Torsional modes.

Radial mode parameter: m	Circumferential mode parameter: n				
	0	1	2	3	4
1	—	224	486	726	961
2	1534	1556	1619	1720	1854
3	3047	3058	3089	3140	3210
4	4565	4571	4592	4626	4676(kHz)

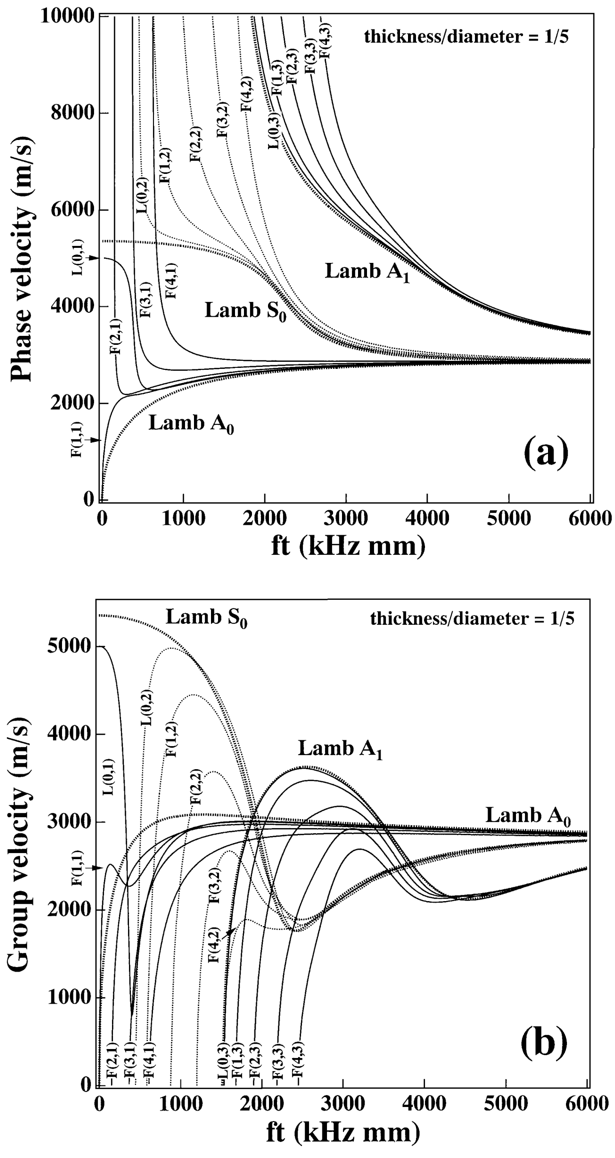

Fig. 2. Phase (a) and group (b) velocity dispersions of the L- and F-modes cylindrical waves propagating in a 5-mm-diameter and 1-mm-thickness aluminum pipe.

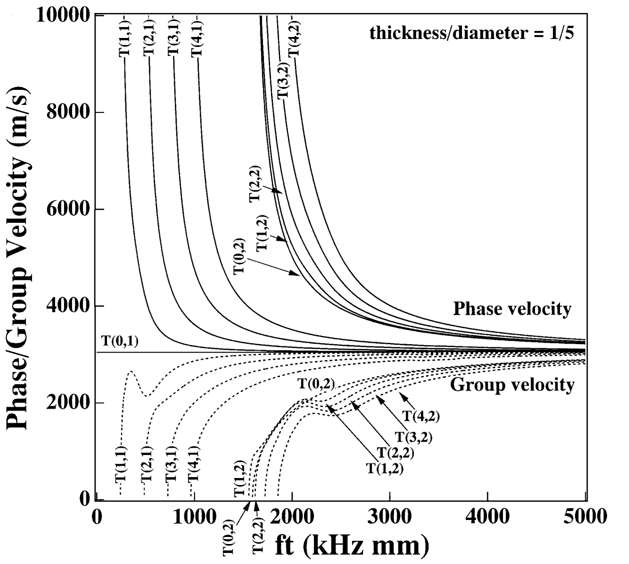

Fig. 3. Theoretical dispersion of phase (solid curves) and group (dotted curves) velocities of the T-mode cylindrical wave propagating in a 5-mm-diameter and 1-mm-thickness aluminum pipe.

axis has to be adjusted. Thus, the horizontal axis in Fig. 2 is normalized by the product of frequency f (in kHz) and wall thickness t (in mm). This behavior is common to that of the Lamb wave dispersion curves.[18)]

Phase and group velocity dispersion of the T-mode (including the higher order circumferential modes) is shown in Fig. 3. Dispersion curves of the T-mode are relatively simple because of coupling mainly with the bulk SH wave, but several modes of group velocity dispersion are not monotonically increased. The T(0, 1) mode is not dispersive because the bulk SH wave is only coupled along the axial direction of the pipe. Phase and group velocities of all the T-modes are identical to the bulk shear wave velocity at large *ft* values on the horizontal axis.

Note that the phase velocity starts to increase sharply as the frequency approaches the cut-off frequency, given in Table I. There is no energy flow along the axial direction at the cut-off frequency. Only the standing waves in the thickness direction exist. This nature is also equivalent to one of the Lamb wave features.

2.2 Variation of dispersion curves for different thicknesses/diameters

We consider, next, effects of thickness/diameter (t/d) ratio on the dispersion curves of the lowest two L-modes. Figures 4(a) and 4(b) show the phase and group dispersion curves of the L(0, 1) and L(0, 2) modes of aluminum pipe for $t/d = 1/2$, 1/3, 1/5, 1/10 and 1/16, respectively. Note that t/d ranges from zero to 1/2 and that $t/d = 1/2$ represents a solid cylinder. Dispersion relations of the A_0 and S_0 mode Lamb waves propagating in an aluminum plate are also shown by thicker solid and dotted curves in Figs. 4(a) and 4(b), respectively. With decreasing t/d values (thinner walled or larger diameter pipes), the dispersion curve of the L(0, 1) mode approaches that of the A_0 mode Lamb wave in a plate whose thickness is equal to the wall thickness t of the pipe. Similarly, the dispersion curve of the L(0, 2) mode approaches that of the S_0 mode Lamb wave. When t/d diminishes ($= > 0$),

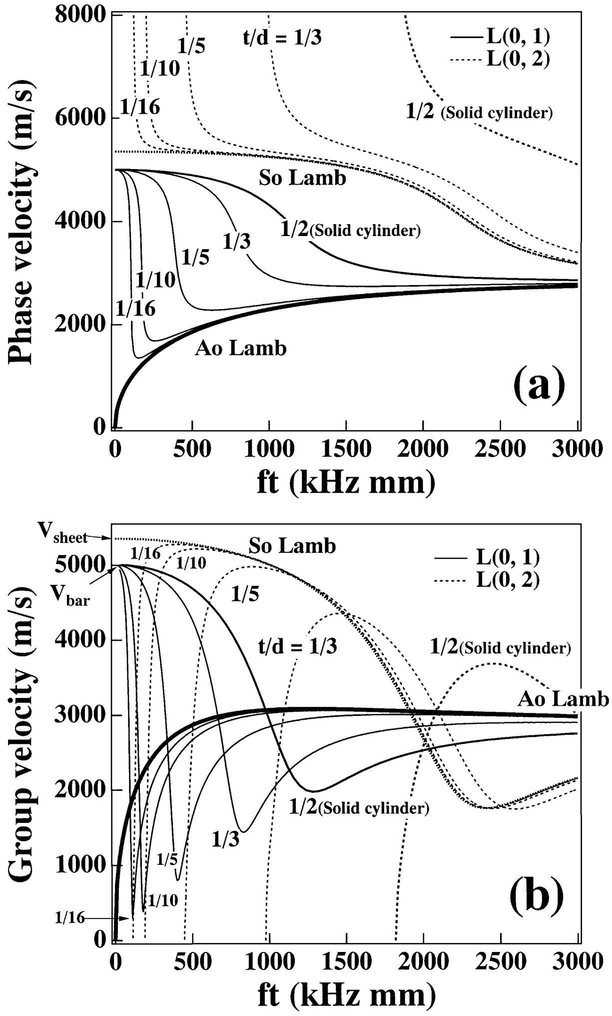

Fig. 4. Phase (a) and group (b) velocity dispersions of the L(0, 1) and L(0, 2) modes for different thickness/diameter of pipes. The dispersion curves of the cylindrical wave gradually approach the Lamb wave dispersions.

L(0, 1) and L(0, 2) modes coincide with the A_0 and S_0 mode Lamb waves because the waveguide is no longer a cylinder but a plate. The dispersion relations of the cylindrical wave were found to have a characteristic feature intermediate between the guided waves propagating in a solid cylinder and a plate.

As shown in Fig. 4(b), the maximum group velocity of the cylindrical wave is dependent on t/d. When $t/d > 1/5$ (for the case of an aluminum pipe; this value depends on the longitudinal and shear wave velocities), the L(0, 1) mode at $ft = 0$ has the maximum group velocity. This velocity is the so-called bar velocity, $v_{\rm bar} = c_t\sqrt{(3c_l^2 - 4c_t^2)/(c_l^2 - c_t^2)}$. For $t/d < 1/5$, the L(0, 2) mode plays the dominant role in determining the maximum group velocity, which is a function of t/d as shown in Fig. 4(b). For $t/d = 0$, the maximum group velocity is equal to the sheet wave velocity, $v_{\rm sheet} = 2c_t\sqrt{1 - (c_t^2/c_l^2)}$, of the Lamb wave. This feature suggests a possibility of estimating the wall thickness of the pipe from the primary wave velocity measurement.[19)]

2.3 Comparison between cylindrical waves and Lamb waves

Similarities between the theoretical dispersions of the

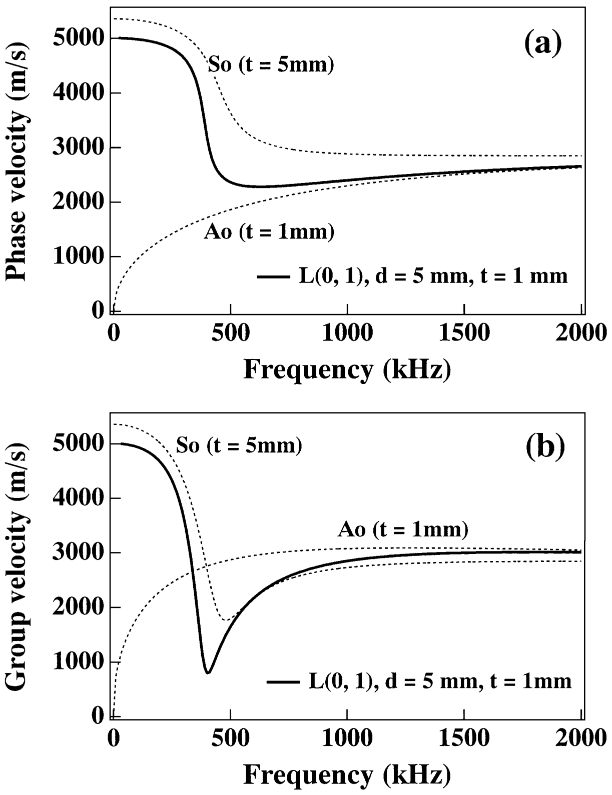

Fig. 5. Phase (a) and group (b) velocity dispersions among the L(0, 1) mode cylindrical wave (5 mm diameter, 1 mm thickness), A_0 (1 mm plate thickness) and S_0 (5 mm plate thickness) mode Lamb waves. The L(0, 1) mode asymptotically approaches the A_0 mode Lamb wave and takes a similar manner of the S_0 mode Lamb wave in a relatively low frequency range.

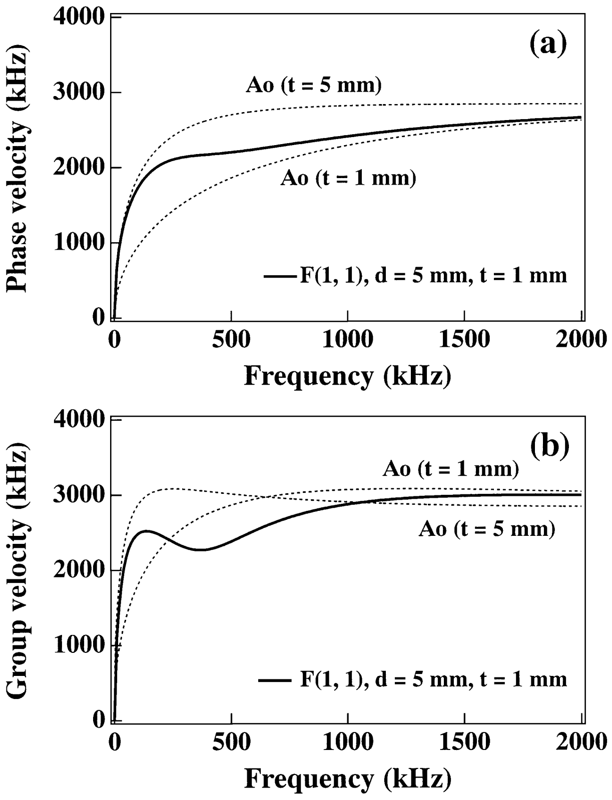

Fig. 6. Phase (a) and group (b) velocity dispersions among the F(1, 1) mode cylindrical wave (5 mm diameter, 1 mm thickness), A_0 (1 mm plate thickness) and A_0 (5 mm plate thickness) mode Lamb waves.

cylindrical and Lamb waves are examined for the L(0, 1) and F(1, 1) modes. Figures 5(a) and 5(b) show the phase and group velocity dispersions (solid lines) of the L(0, 1) mode of aluminum pipe of 5 mm diameter and 1 mm wall thickness. Dispersion curves of the S_0 and A_0 Lamb waves for 5-mm and 1-mm-thick plates are also given as dotted curves in Figs. 5(a) and 5(b), respectively. The L(0, 1) mode is axially symmetric and takes uniform displacement along the circumference on the entire pipe. However, the wall itself vibrates antisymmetrically, similar to the A_0 Lamb wave. Therefore, the dispersion of the L(0, 1) mode is similar to that of the S_0 Lamb waves for a 5-mm-thick plate in the low frequency range, while it asymptotically approaches the dispersion of the A_0 mode propagating on a 1-mm-thick plate in the higher frequency range, in lieu of approaching the S_0 mode, as shown in Figs. 5(a) and 5(b). In contrast to this L(0, 1) mode behavior, the F(1, 1) mode produces the pipe vibration of antisymmetrical nature; that is, the entire pipe segment moves up and down. Additionally, the pipe wall translates similarly without thickness changes. Thus, the F(1, 1) mode asymptotically approaches the two dispersion curves of the A_0 mode. In the low frequency range, the dispersion curves of the F(1, 1) mode and A_0 mode Lamb waves propagating on a 5-mm-thick plate merge together. In the high frequency range, the dispersion curves of the F(1, 1) mode and A_0 mode Lamb waves propagating on a 1-mm-thick plate tend to coincide. These trends are shown in Figs. 6(a) and 6(b).

The above observation indicates that the dispersion relation for the phase velocity of the L(0, 1) and F(1, 1) modes has the characteristics that are bounded by the two Lamb wave dispersions of plates with the thickness identical to the diameter or the wall thickness of the pipe. The dispersion relation for the group velocity can be similarly considered, except that the cylindrical velocity swings out in the intermediate frequency range.

3. Experimental Verification of Dispersion Behavior

The dispersion behavior of the cylindrical waves is evaluated experimentally and compared to theoretical prediction. Laser ultrasonic methods were utilized for wide band excitation[20] and for detection[21] in the experiment. Schematic illustration of the present experiment is shown in Fig. 7. An aluminum pipe of 5 mm diameter, 1 mm thickness and 1000 mm length was used as a specimen. A Q-switched Nd:YAG pulse laser (Continuum, NY60) was employed to excite cylindrical waves. Laser wavelength, beam diameter, pulse duration and energy were 1064 nm, 5 mm, 5 ns and 10 mJ, respectively. The laser beam was tightly focused on the center of the wall thickness at the pipe end by a single plano-convex lens with a focal length of 50 mm (see Fig. 7). The circumferential beam position was at an angle θ from the reference position. In the setup, laser excitation utilizes the plasma effect[20] and a compressive moment is driven at the irradiated position. The cylindrical waves were detected by a heterodyne Mach-Zehnder laser interferometer (BMI, SH-140) having a 20 MHz flat bandwidth with a frequency-doubled Nd:YAG CW laser as a probe beam. The position of the probe beam was fixed at $\theta = 0°$ in the circumference and $z = 300$ mm in the wave propagation length from the pipe end in all experiments. Detected signals of the cylindrical waves were

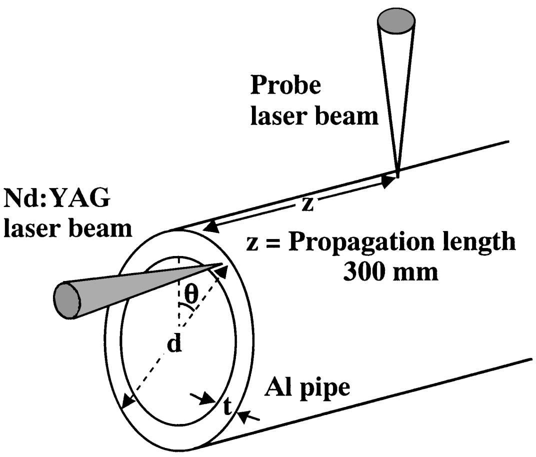

Fig. 7. Schematic illustration of the experiments. Diameter and thickness of the aluminum pipe were 5 mm and 1 mm, respectively. Propagation length z of the cylindrical waves were set to be 300 mm.

recorded using a digitizer (Tektronix, RTD720A) with a 40 ns sampling interval.

In the first experiment, the position of the excitation laser beam was fixed at $\theta = 0°$. Figure 8 shows a typical time domain signal of the cylindrical waves detected. We can divide the signal into two regions on the basis of arrival time of the bulk shear wave. The boundary between the two regions located at 98.7 μs is shown as a vertical line in Fig. 8. From the calculated group velocity data in Fig. 2(b), the initial fast-arrival region consists of the components of the L(0, 1), L(0, 2), F(1, 2), F(2, 2), L(0, 3), F(1, 3) and F(2, 3) modes, because their group velocities are higher than the bulk shear wave velocity (3040 m/s). Large amplitude and low frequency components characterize the following slow-arrival region starting at ∼110 μs. Other higher frequency modes are present as well. The slow-arrival region is mainly due to the F(1, 1) mode vibration as shown in the following time-frequency analysis. Those arriving at 100–110 μs correspond to the L(0, 1), F(1, 1) and F(2, 1) modes. Gray-scale representation of wavelet coefficients for the time domain signal (Fig. 8) as functions of both group velocity and frequency is shown in Figs. 9(a)–9(c). The wavelet coefficients are represented in the range of 0 to −15 dB in Figs. 9(a) and 9(b)

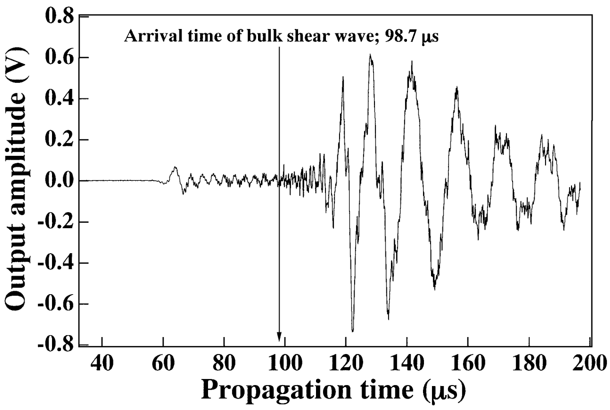

Fig. 8. Time domain signal of the cylindrical wave propagating along a 5-mm-diameter and 1-mm-thickness aluminum pipe. Arrow indicates arrival time of bulk shear wave ($c_t = 3040$ m/s).

and in the range of 0 to −10 dB in Fig. 9(c). Gabor function was used as the mother-wavelet to calculate the wavelet coefficient.[22] The corresponding propagation time is also shown in the right axis in Fig. 9. The peak power of the wavelet coefficient was located at 52.3 kHz of the F(1, 1) mode and was set to be 0 dB for relative comparison. To compare with the theory, the L(0, 1), F(1, 1), F(1, 2), F(2, 1), F(2, 2) and F(3, 2) modes of theoretical dispersions are superimposed on the experimental results in Figs. 9(b) and 9(c). Dispersion curves of the T-modes are omitted in Fig. 9. This is because the laser interferometer has only the sensitivity for out-of-plane displacement and cannot detect the T-modes. The experimental results coincide well with the theoretical velocity dispersions. The F(1, 1) mode was the most efficiently excited wave in the present experiment. However, generation efficiency for each mode is strongly dependent on *initial-value-problem* of cylinder wave generation, *e.g.* time and spatial distributions of a generation source. The amplitude of the L(0, 1) or F(2, 1) mode was the next largest (larger than −10 dB from the peak), and that of the L(0, 2), F(1, 2) or F(2, 2) mode took a value between −15 dB and −10 dB.

The cylindrical waves generated by laser irradiation at five different circumferential positions ($\theta = 0$, 45, 90, 135 and 180°) are shown in Fig. 10. Both the amplitudes and polarities of the fast-arrival region including peak a were almost independent of θ. In contrast, the polarity of large amplitude portions especially peak b, primarily due to the F(1, 1) mode, changed at $\theta = 90°$ and the amplitude was the smallest at $\theta = 90°$ (in fact, buried in other unidentified high-frequency modes). This is because the out-of-plane displacement of the F(1, 1) mode in the circumference is represented by a cosine function. Figure 11 shows a schematic illustration of F(1, 1) mode vibration in a cross-sectional view. When the irradiation position θ takes a value of 0° or 90°, the maximum or minimum amplitude, respectively, of vibration is obtained by the laser interferometer. Figure 12 shows the amplitude ratio of peak b to peak a [or F(1, 1)/L(0, 1)] as a function of θ. Closed circles indicate experimental data. At $\theta = 90°$, the error bar is inserted because no clear peak was detectable. The solid curve represents 8.8 cos θ. Coefficient 8.8 was determined by least-squares-fit for the experimental results. This fit shows good agreement between the experiment and theory.

4. Conclusion

We evaluated the theoretical dispersion of the cylindrical waves and showed characteristics of the phase and group velocity dispersions.

(1) The higher order circumferential T-modes are defined and a rationalized classification scheme of the L-, F- and T-modes is proposed. It is shown that the L- and F-modes are the guided wave equivalent of the Lamb wave, and the T-mode is the guided wave equivalent of the SH mode plate wave.

(2) Various modes of the cylindrical wave had characteristic features bounded by those of the guided wave propagating along a solid cylinder and plate or by the Lamb wave modes.

Wide-band excitation of the cylindrical waves was experimentally carried out using the laser ultrasonic methods. Time-frequency analyses of the cylindrical waves using the

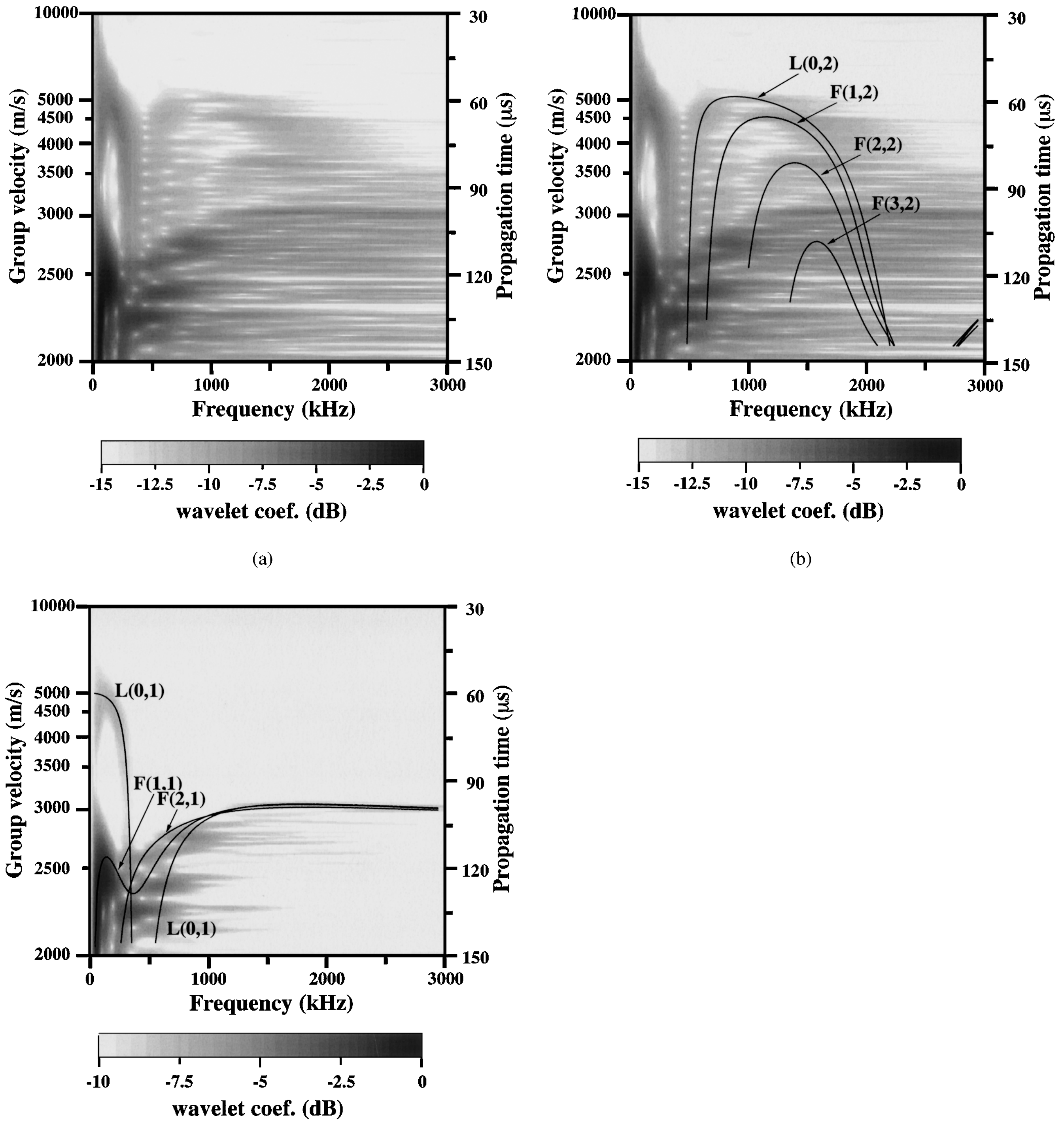

Fig. 9. Wavelet coefficients as functions of group velocity and frequency calculated from the time domain signal of Fig. 8. (a) Gray scale representation from peak to -15 dB. (b) theoretical dispersions of the L(0, 2), F(1, 2), F(2, 2) and F(3, 2) were superimposed on the wavelet coefficient. (c) Gray scale was from peak to -10 dB to compare with theoretical dispersion of the L(0, 1), F(1, 1) and F(2, 1) modes.

wavelet transform were used to verify the theoretical dispersion curves. Experimental dispersion agreed well with the theoretical dispersion for the L(0, 1), F(1, 1), F(2, 1), L(0, 2), F(1, 2) and F(2, 2) modes of the cylindrical waves.

1) M. G. Silk and K. F. Bainton: Ultrasonics **17** (1979) 11.
2) D. N. Alleyne and P. Cawley: *Review of Progress in Quantitative Nondestructive Evaluation*, eds. D. O. Thompson and D. E. Chimenti (Plenum, New York, 1995) Vol. 14, p. 2073.
3) D. N. Alleyne and P. Cawley: J. Nondestr. Eval. **15** (1996) 11.
4) D. N. Alleyne and P. Cawley: Mater. Eval. (1997) 504.
5) M. J. S. Lowe, D. N. Alleyne and P. Cawley: Ultrasonics **36** (1998) 147.
6) J. E. Greenspon: J. Acoust. Soc. Am. **32** (1960) 1017.
7) J. E. Greenspon: J. Acoust. Soc. Am. **33** (1961) 1321.

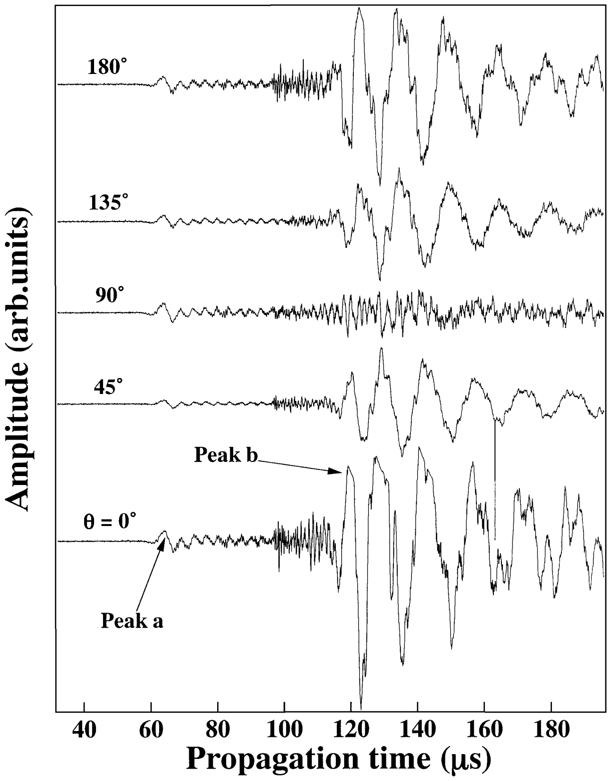

Fig. 10. Time domain signals of cylindrical waves for five different irradiation positions θ (=0, 45, 90, 135 and 180°).

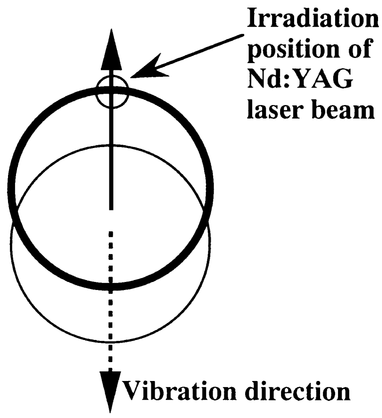

Fig. 11. Vibration direction of the F(1, 1) mode. When $\theta = 0°$, the detected signal takes the maximum amplitude. Otherwise, it takes a minimum when $\theta = 90°$.

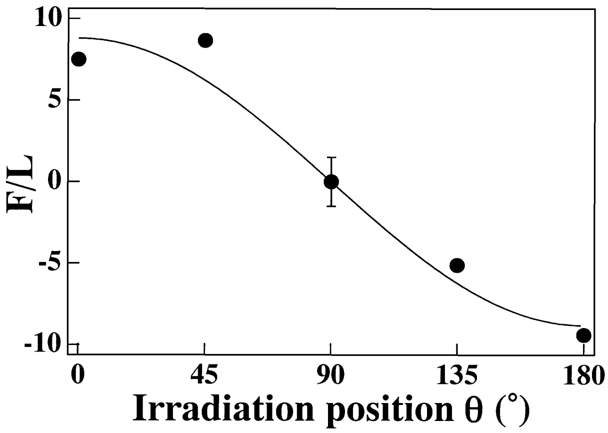

Fig. 12. Amplitude ratio of the F(1, 1) mode to L(0, 1) mode as a function of irradiation position θ of Nd:YAG laser beam. Solid circles indicate experimental data. Solid curve is a cosine function based on the theoretical circumferential displacement.

8) J. L. Rose, Y. Cho and J. J. Ditri: *Review of Progress in Quantitative Nondestructive Evaluation*, eds. D. O. Thompson and D. E. Chimenti (Plenum, New York, 1994) Vol. 13, p. 259.
9) J. L. Rose, J. J. Ditri, A. Pilarski, K. Rajana and F. Carr: NDT & T Int. **27** (1994) 307.
10) H. Nishino, F. Uchida, S. Takashina, M. Takemoto and K. Ono: EWGAE 2000, 24th Europian Conf. Acoustic Emission Testing, 2000, p. 139.
11) D. C. Gazis: J. Acoust. Soc. Am. **31** (1959) 568. There is an error in C_{31} term of the 6×6 matrix frequency equation (19) (first α_1 should be changed into a).
12) A. H. Fitch: J. Acoust. Soc. Am. **35** (1963) 706.
13) This mode should be F(1, 2) mode in our classification.
14) B. A. Auld: *Acoustic Fields and Waves in Solids* (Krieger, Florida, 1990) 2nd ed., Vol II.
15) A. H. Meitzler: J. Acoust. Soc. Am. **33** (1961) 435.
16) J. Zemanek: J. Acoust. Soc. Am. **51** (1972) 265.
17) D. Royer and E. Dieulesaint: *Elastic Waves in Solid I, Free and Guided Propagation* (Springer-Verlag, Berlin, Heidelberg, New York, 2000).
18) I. A. Viktrov: *Rayleigh and Lamb Waves*, (Plenum, New York, 1967).
19) H. Nishino, F. Uchida, M. Takemoto and K. Ono: to be submitted to Appl. Phys. Lett.
20) D. A. Hutchins: *Ultrasonic Generation by Pulsed Laser*, eds. W. P. Mason and R. N. Thurston (Academic, New York, 1988) Physical Acoustics XVIII.
21) G. I. Stegeman: IEEE Trans. Son. & Ultrason. **23** (1976) 33.
22) for example as a dispersion analysis, H. Cho, S. Ogawa and M. Takemoto: NDT & E Int. **29** (1996) 301.